Determination of optical gain and absorption of quantum dots with an improved segmented contact method

Y.-C. Xin, H. Su and L. F. Lester
Center for High Technology Materials, University of New Mexico
1313 Goddard SE, Albuquerque, NM 87106
Tel. (505) 272-7868, Fax. (505) 272-7801, e-mail: ycxin@chtm.unm.edu

L. Zhang, A. L. Gray, S. Luong, K. Sun, Z. Zou, T. Whittington, J. Zilko and P. M. Varangis
Zia Laser, Inc., Albuquerque, NM 87106

ABSTRACT

For understanding the fundamental processes in QDs and optimizing the design of QD optical devices, it is essential to obtain accurate optical gain and absorption spectra. An improved segmented-contact method is described that subtracts the unguided spontaneous emission that normally introduces error into the calculated gain and absorption. Using the technique a QD gain spectrum is measured to an accuracy of less than 0.2/cm at nominal gain values below 2/cm. This capability also enables precise measurement of waveguide internal loss, unamplified spontaneous emission spectra and Stark shift data.

Keywords: Quantum dots, optical gain, segmented contact method, spontaneous emission

INTRODUCTION

Quantum dot (QDs) lasers have attracted attention due to their superior lasing characteristics compared to conventional quantum well (QW) lasers, including low-threshold current density[1,2] and a small linewidth enhancement factor[3]. For understanding the fundamental processes in QDs and optimizing the design of QD optical devices, such as DFB lasers and VCSELs that have generally larger loss than Fabry-Perot devices, it is essential to obtain accurate gain and absorption spectra. In the past, the segmented contact method was successfully used to measure the gain and absorption of quantum well materials by analyzing the edge-emitted amplified spontaneous emission spectra (ASE) [4]. In the standard data reduction of results from the segmented-contact method, unguided spontaneous emission due to leakage currents and weak waveguiding is not treated, which introduces error into the calculated gain and absorption. Such error cannot be ignored in quantum dot devices due to their smaller modal gain (10-20/cm) and loss values. Other researchers have proposed ways of eliminating these errors but they tend to be relatively complex.[5] In this paper, we describe an improved segmented contact method that is simple to implement by manipulating the data from single, double, and triple biased sections. The new approach essentially subtracts background signals from the measurement and results in clean and accurate gain and absorption spectra. From this self-calibrating method, a quantum dot gain spectrum is measured to an accuracy of less than 0.2/cm at nominal gain values below 2/cm. Other optical parameters determined with the technique such as pure spontaneous emission and the quantum confined Stark effect are also described.

DEVICE STRUCTURES, GROWTH AND TEST

1. Device structure and growth

The segmented contact devices were processed from a multi-layer dots-in-a-well (DWELL) laser structure consisting of 6 stacks of dots. The DWELL laser structure was grown by elemental source molecular beam epitaxy (MBE) on an n^+-doped, <100> oriented GaAs substrate. The epitaxial layers consist of an n-type (10^{18} cm^{-3}) 300-nm-thick GaAs buffer, an n-type lower $Al_{0.7}Ga_{0.3}As$ cladding layer, a 315-nm-thick GaAs waveguide including the laser active region, a p-type

Physics and Simulation of Optoelectronic Devices XIII, edited by Marek Osinski,
Fritz Henneberger, Hiroshi Amano, Proc. of SPIE Vol. 5722 (SPIE, Bellingham, WA, 2005)
0277-786X/05/$15 · doi: 10.1117/12.591241

upper cladding layer, and a p-doped (3×10^{19} cm^{-3}) 60-nm-thick GaAs cap. The cladding layers are doped at 10^{17} cm^{-3} and are each 2 μm thick. In the center of the waveguide, 6 DWELL layers with 29 nm GaAs barriers were grown. QDs with an equivalent coverage of approximately 2 monolayers of InAs are confined in the middle of a 10 nm thick $In_{0.15}Ga_{0.85}As$ QW in each layer. The QDís and QW were typically grown at 500 °C, as measured by an optical pyrometer. The QDís formed under these conditions have an areal density of about 3×10^{10} cm^{-2}, a base diameter <40nm, and are 7 nm high. Detailed descriptions of the DWELL growth technique can be found elsewhere.[11, 12, 13]

GaAs	p 3^{19}	60nm	
$Al_{.7->0}GaAs$	p 2^{19}	18nm	
$Al_{.7}Ga_{.3}As$	p 1^{17}	2000nm	
GaAs		26nm	
GaAs		29nm	6X
InAs/ $In_{.15}Ga_{.85}As$		10nm	
GaAs		55nm	
$Al_{.7}Ga_{.3}As$,	n1^{17}	2000nm	
$Al_{0->.7}GaAs$	n6^{17}	18nm	
GaAs	n 1^{18}	300nm	
GaAs N+ 2" substrate			

Figure 1. Structure of the 6-stack DWELL laser

2. Device processing

The wafer was processed into 3-μm wide and deep-etched ridge waveguides with 16 segmented-contact sections. Each section is 0.5 mm and the optical cavity length is 8 mm. The processing recipe is outlined in Figure 2:

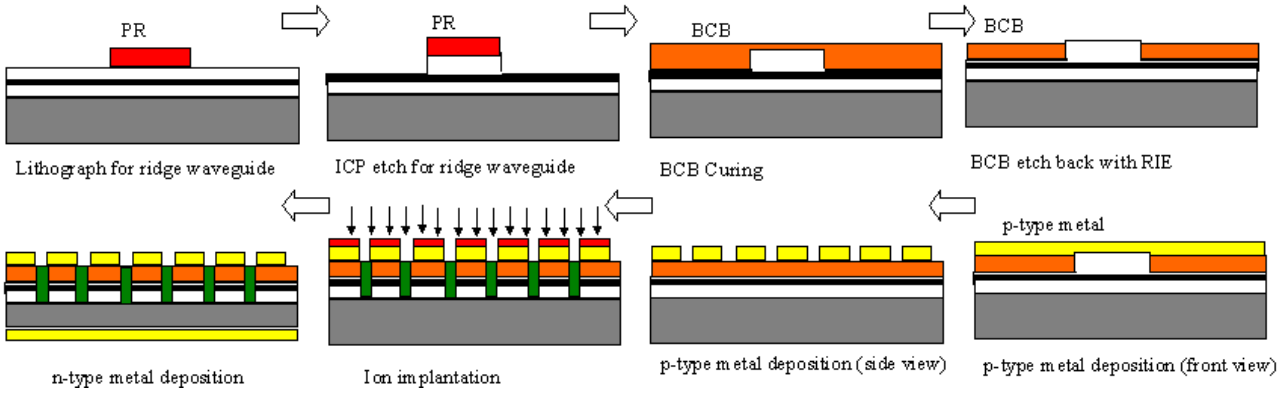

Figure 2. Process flow for the segmented-contact device

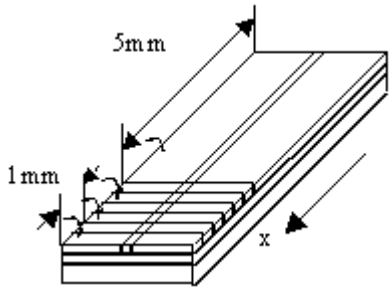

Figure 3. Structure of segmented contact device

After the first lithography step, the sample was etched to form 3-μm wide and 1.8-μm deep ridges in BCl_3 inductively coupled plasma. Then standard BCB processing was applied for planarization and to isolate the p-type metal and the etched upper cladding layer. A segmented-contact mask was used to define the p-type metal contact and ion implant isolation. After lapping and polishing of the substrate, Au/Ge/Ni/Au n-type metallization was deposited, and the sample was annealed at 380°C for 1 minute. The first 6 sections of device were wire bonded to form three 1-mm-sections, and the last 10 sections were wire bonded together to form one 5-mm absorption section, as shown in Figure 3.

3. The net modal gain and loss measurement system

The net modal gain and loss measurement system consists of two blocks: the current pump system and the signal collection system shown in Figure 4. Each 1-mm section has its own CW current source, and a multimeter is used to monitor the pump current. A reverse bias of 7 V is applied to the absorption section to minimize reflection from back facet. Device is mounted on an AlN heatsink, and a TE cooler controls the temperature at 25C°. The emission from the device is collected into a monochrometer by two lenses. A polarizer is placed between the first lens and a chopper to filter out the TM mode emission. An InGaAs detector cooled to 213K converts the light to an electrical signal. The latter is then boosted by a lock-in amplifier and collected by a computer. For the optical gain calculation, the ASE spectra from the first section (referenced from the front emitting facet), I_L, both the first and second sections, I_{2L},, and then all 3 sections, I_{3L} are measured. All three pumping scenarios use the same current density. For the absorption calculation, I_{3L} is replaced by I_{31}, a measurement of the ASE with the first and third sections pumped under the same current density and a reverse bias voltage applied to the second (absorber) section.

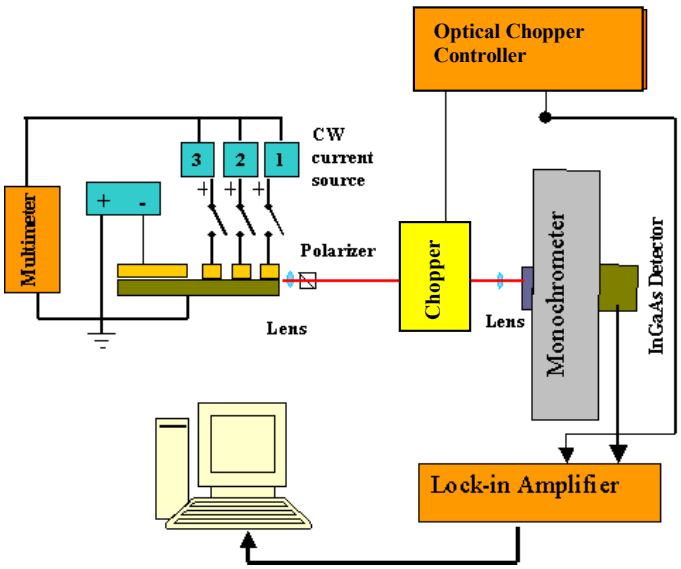

Figure 4. Schematic diagram of the net modal gain and loss measurement system for the segmented contact DUT.

DERIVATION AND ANALYSIS

1. Gain measurements

The net modal gain, G, the differential change in the amplified spontaneous emission (ASE) intensity with the transmission length, dI/dx, and the pure (unamplified) spontaneous emission, S, are related by the following equation: [6]

$$\frac{dI}{dx} = GI + S \tag{1}$$

G is related to the material gain g, internal loss α_i, and optical confinement factor Γ by $G = \Gamma g - \alpha_i$. Using the boundary conditions that $I=0$ at $x=0$, the following expression can be derived: [7]

$$I = \frac{S}{G}\left(\exp(G \cdot x) - 1\right) \tag{2}$$

From equation 2, G can be obtained by measuring the ASE emitted from cavities with different pumping lengths. Using two judiciously chosen bias configurations, the net modal gain G can be calculated by the standard segmented-contact method:[4]

$$\begin{aligned} I_L &= \frac{S}{G}\left(\exp(G \cdot L) - 1\right) \\ I_{2L} &= \frac{S}{G}\left(\exp(G \cdot 2L) - 1\right) \end{aligned} \tag{3}$$

Here $I_L\,(x=L)$ is the ASE intensity when the first section is pumped, $I_{2L}\,(x=2L)$ is the ASE intensity when both the first and second sections of equal length are pumped, and L is the length of one section. The relation between I_L, I_{2L}, G and S can be written as:

$$\frac{I_{2L}}{I_L} = \frac{\frac{S}{G}\left(\exp(G \cdot 2L) - 1\right)}{\frac{S}{G}\left(\exp(G \cdot L) - 1\right)} = \exp(G \cdot L) + 1 \tag{4}$$

The net modal gain G can be calculated by: [4]

$$G = \frac{1}{L}\ln\left(\frac{I_{2L}}{I_L} - 1\right) \tag{5}$$

However, in this familiar method, the unguided spontaneous emission is ignored, which can introduce error into the gain and absorption data. One possible source for the unguided spontaneous is leakage current or weak waveguiding in the device. For a quantum well (QW) gain medium, such error can frequently be ignored given the relatively large gain of a QW sample. For a QD sample, however, in which the gain and loss are much smaller than in the QW, this error cannot be ignored and the unguided spontaneous emission has to be treated. The relation between the ASE intensity and optical gain can be rewritten as

$$I = \frac{S}{G}\left(\exp(G \cdot x) - 1\right) + I_{leak} \tag{6}$$

Here the I_{leak} is the unguided spontaneous emission intensity. For the upgraded segmented contact method, the ASE spectra when pumping the first section, $I_L\,(x=L)$, both the first and second sections, $I_{2L}\,(x=2L)$, and all 3 sections, I_{3L} $(x=3L)$, are measured with same pump current density.

$$I_L = \frac{S}{G}\left(\exp(G \cdot L) - 1\right) + I_{leak-1}$$
$$I_{2L} = \frac{S}{G}\left(\exp(G \cdot 2L) - 1\right) + I_{leak-2} \quad (7)$$
$$I_{3L} = \frac{S}{G}\left(\exp(G \cdot 3L) - 1\right) + I_{leak-3}$$

For the device geometries described above, most of the unguided spontaneous emission from section 2 and section 3 will be absorbed or scattered before the coupling lens can collect it. Section 1 is the dominant source of unguided spontaneous emission. It is a reasonable approximation that I_{leak} is same for the different pumping configurations described above. Therefore:
:

$$\frac{I_{3L} - I_L}{I_{2L} - I_L} = \frac{\exp(3GL) - \exp(GL)}{\exp(2GL) - \exp(GL)} = \exp(GL) + 1 \quad (8)$$

A simple expression for the net modal gain G is obtained as:

$$G = \frac{1}{L}\ln\left(\frac{I_{3L} - I_L}{I_{2L} - I_L} - 1\right) \quad (9)$$

With equation (9), the background signals are subtracted from the measurement and the result is a clean, accurate gain spectrum. The result of the net modal gain under different pump current densities is shown in Figure 5.

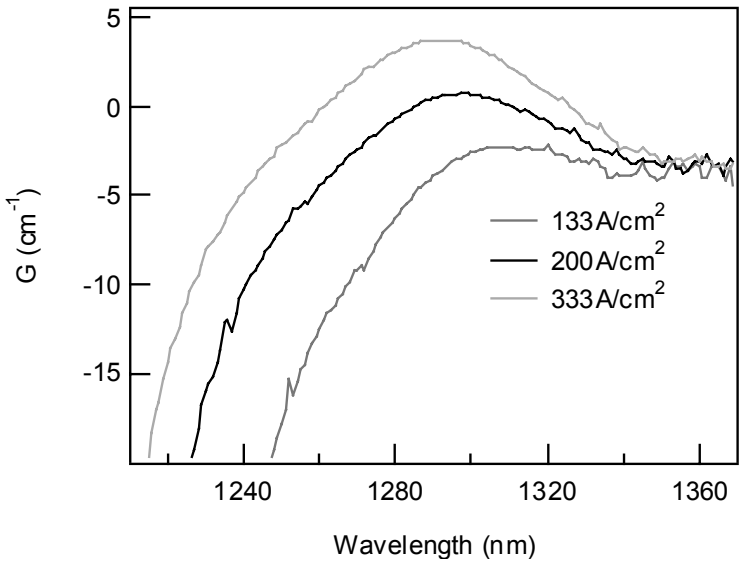

Figure 5. Net modal gain spectra of the QD sample measured with the improved segmented-contact method.

To check the accuracy of the improved technique, we can compare the data with laser threshold measurements. When all sections are pumped together, the device operates as a 8-mm cavity length semiconductor laser in which the net

modal gain equals the mirror loss at threshold. We find that the 8-mm cavity length ridge laser emits at 1294 nm and the threshold current density is 275 A/cm^2. A mirror loss of 1.42/cm is calculated assuming a mirror reflectivity of 32%. Figure 6 shows the net modal gain spectrum at a current density of 275 A/cm^2 measured with the improved segmented contact method for comparison. The laser data is also shown as a single point in Figure 6. Under the same current density, the peak of the gain spectrum using the improved segmented contact method is 1.21/cm at a wavelength of 1294 nm. This data shows that the new method is accurate to about 0.2/cm.

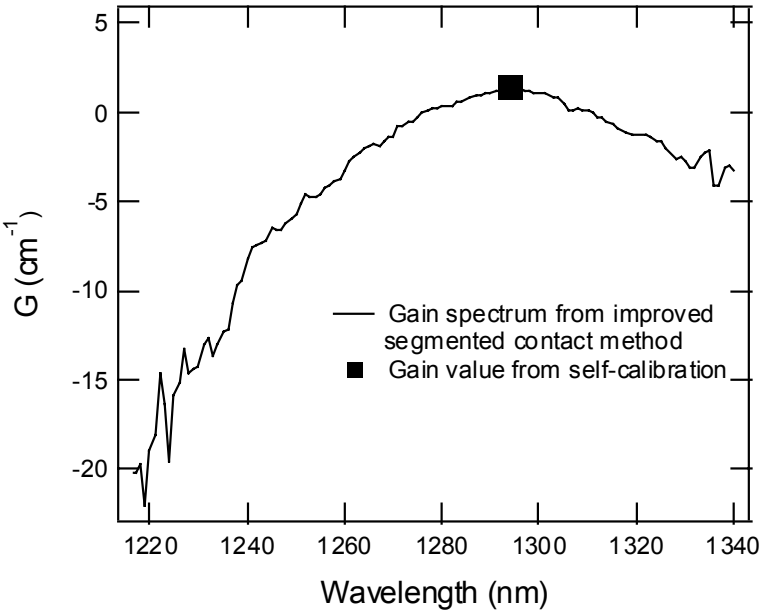

Figure 6. Net modal gain of QD sample under a pump current density of 275A/cm^2.

2. Absorption measurements

The modal absorption α, the transmitted intensity I_t, the initial ASE intensity I, and the transmission length L are related by the follow equation:

$$I_t = I \exp(-\alpha \cdot L) \tag{10}$$

In the standard segmented-contact absorption method, α is found by measuring the ASE from pumping the first section only (I_1) and then pumping only the second section under the same current density while converting the first section to an absorber of length L. The absorption α can be calculated with the equation:[4]

$$\alpha = \frac{1}{L} \ln\left(\frac{I_1}{I_2}\right) \tag{11}$$

There is a similar issue that the unguided spontaneous emission will introduce error into the absorption calculation, and such error cannot be ignored in quantum dot materials due to their smaller loss values. To eliminate this problem, the ASE intensity with only the first section biased, I_1 (x=L), with both the first and second sections biased, I_{21} (x=$2L$), and with the first and third sections pumped and the second section absorbing, I_{31}, are measured. Assuming that the leakage signal I_{leak} is the same for the 3 different pumping configurations, the following equations are derived:

$$
\begin{aligned}
I_1 &= \frac{S}{G}\left(\exp(G\cdot L)-1\right)+I_{leak} \\
I_{21} &= \frac{S}{G}\left(\exp(G\cdot 2L)-1\right)+I_{leak} \\
I_{31} &= \frac{S}{G}\left(\exp(G\cdot L)-1\right)\exp\left((G-\alpha)\cdot L\right) \\
&\quad + \frac{S}{G}\exp(G\cdot L)-\frac{S}{G}+I_{leak}
\end{aligned}
\tag{12}
$$

So

$$
\frac{I_{21}-I_{31}}{I_{31}-I_1} = \exp(\alpha L) \tag{13}
$$

The absorption α will be calculated by followed equation

$$
\alpha = \frac{1}{L}\ln\left(\frac{I_{21}-I_1}{I_{31}-I_1}\right) \tag{14}
$$

With equation (14), the background signals were subtracted from the measurement and the result is a more accurate absorption spectrum. The QD modal absorption spectra under different reverse bias conditions is shown as Figure 7. The waveguide internal loss can be read from the absorption spectrum[4] at long wavelength as 3.3/cm.

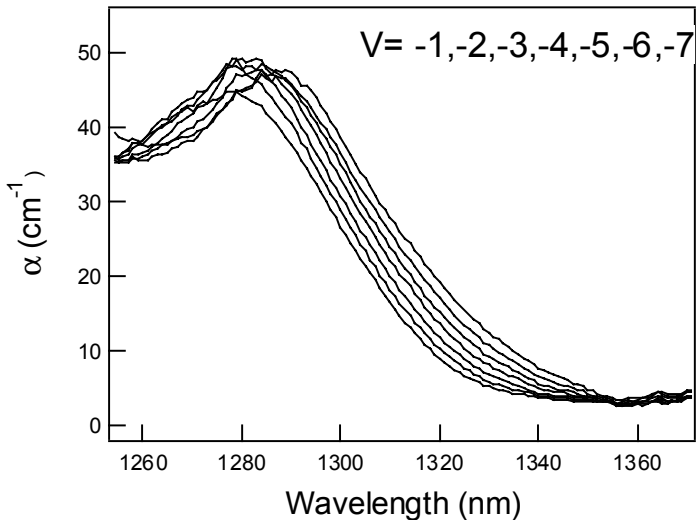

Figure 7. Modal absorption spectra under different reverse bias conditions

To check the accuracy of the absorption spectra, a comparison using data from a multi-section laser can be used. When the 8-mm cavity is uniformly pumped except the second section is short-circuited to ground, the device lases at a wavelength of 1293 nm, and a threshold current density in the pumped sections of 666 A/cm^2 is measured as displayed in Figure 8.

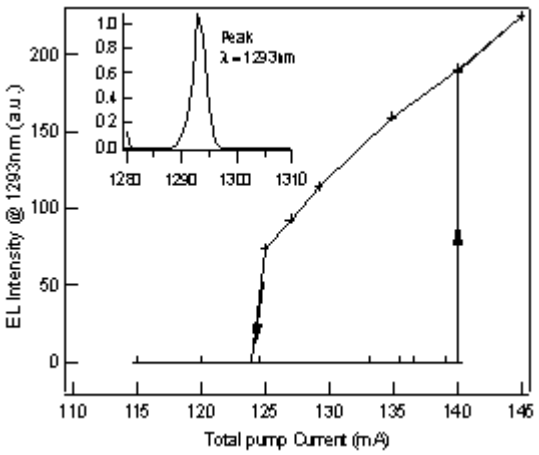

Figure 8 L-I curve and spectrum with second section grounded

At threshold, the relationship between net modal gain and modal absorption in the multi-section laser is:

$$G \cdot L_{active} = \alpha \cdot L_{absorb} + \alpha_m \cdot (L_{absorb} + L_{active}) \tag{15}$$

For the device geometries described above, L_{active} is 7-mm and L_{absorb} is 1-mm. The modal absorption and the net modal gain spectra are calculated by equation (9) and equation (14) at a current density of 666 A/cm^2 in the gain sections and 0 Volts on the absorber. The results are shown in Figure 9. From the net modal gain spectrum, G was read to be 6.3/cm at 666 A/cm^2 and 1293 nm wavelength. With this G value and equation (15), α was calculated to be 32.7/cm. From the spectrum of absorption in Figure 9, α is read as 33.4/cm, showing a good agreement.

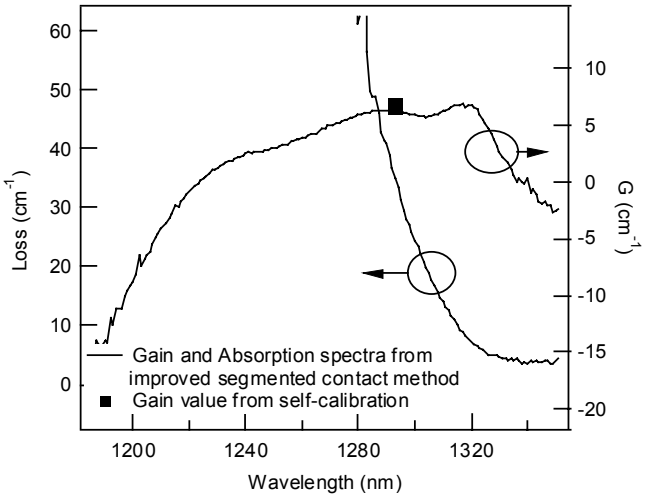

Figure 9. Net modal gain and absorption under a current density of 20 mA/section in the gain sections and 0 V bias on the absorber.

3. Unamplified electro-spontaneous spectra

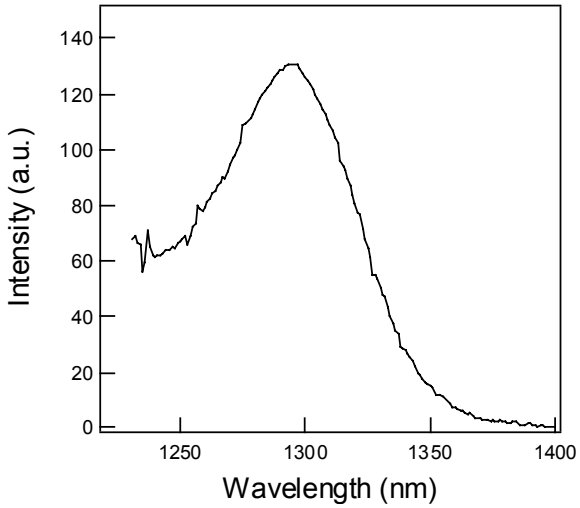

Figure 10 Unamplified electro-spontaneous emission spectrum under current density of 6mA/section

From equation (7) and assuming that the I_{leak} is the same for the different pumping configurations, the ASE intensity, the unamplified SE intensity and the net modal gain are related as:

$$I_{2L} - I_L = \frac{S}{G}\left[\exp(G \cdot L) - 1\right]\exp(G \cdot L) \tag{16}$$

Rearrangin, the unamplified spontaneous emission intensity S is related to the ASE intensity measured under bias conditions I_L and I_{2L} and the net modal gain G by:

$$S = G\frac{I_{2L} - I_L}{\left(\exp(G \cdot L) - 1\right)\exp(GL)} \tag{17}$$

In this improved segmented-contact method, an accurate spectrum of net modal gain G can be obtained and this allows us to obtain an unamplified spontaneous emission spectra as well. An example of unamplified spontaneous emission data as a function of wavelength calculated using equation (17) appears in Figure 10.

4. Quantum Confined Stark Effect

To explore the electro-absorption effect further, the absorption spectra were measured under different reverse bias conditions by the method described above and shown in Figure 7. In Figure 7, the absorption spectra peaks red-shift to a smaller photon energy when the reverse bias increases. The undoped waveguide and active region of the multilayer quantum dot laser structure wafer is about 315 nm. Assuming all reverse voltage drops across the undoped region, the ground state absorption peak positions were plotted against the reverse bias electric fields in Figure 11. The peak positions at different reverse bias can be described approximately by a linear dependence and the red-shift step is about 1.5 meV/V at a reverse bias of |V|>1V, which deviates from the quadratic dependence and possibly because the field was large enough to begin dissociating the electron-hole pair and thus the transition energy was influenced.[8, 9] The Stark shift has an amplitude of 9.8 meV under an electric field of 150 kV/cm and this is comparable to the measurement of an InAs QD on GaAs.[10]

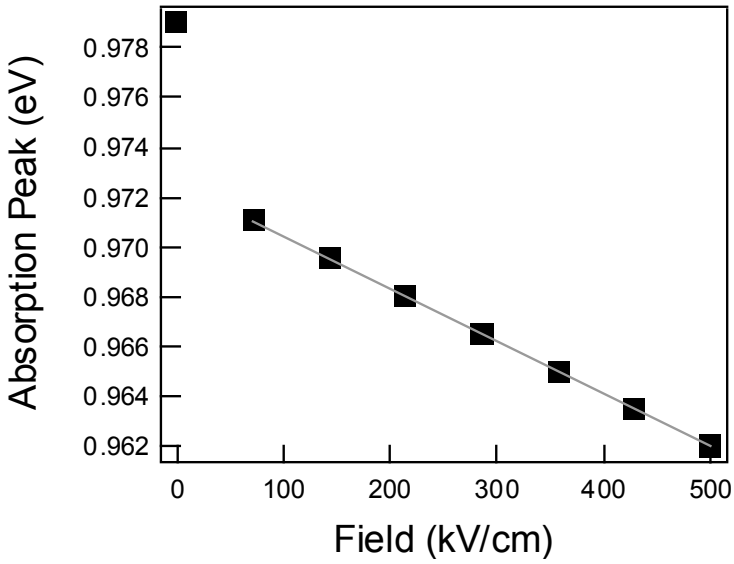

Figure 11 Modal absorption spectrum peak positions under different reverse bias conditions

CONCLUSION

An improved segmented contact method for the net modal gain and absorption measurement was introduced. With this simple method, the background light signals are subtracted from the measurement and a clean and accurate gain or absorption spectra was obtained to an accuracy within 0.2/cm. The unamplified spontaneous emission spectrum was also calculated from the ASE spectra and the net modal gain as a function of wavelength. The QCSE has been observed in these QDs, and the redshift has a linear dependence with reverse bias.

REFERENCES

1. D. L. Huffaker, G. Park, Z. Zou, O. B. Shchekin, and D. G. Deppe, "1.3 mu m room-temperature GaAs-based quantum-dot laser," *Applied Physics Letters* **73**, 2564-2566, 1998.
2. G. T. Liu, A. Stintz, H. Li, K. J. Malloy, and L. F. Lester, "Extremely low room-temperature threshold current density diode lasers using InAs dots in In0.15Ga0.85As quantum well," *Electronics Letters* **35**, 1163-1165, 1999.
3. T. C. Newell, D. J. Bossert, A. Stintz, B. Fuchs, K. J. Malloy, and L. F. Lester, "Gain and linewidth enhancement factor in InAs quantum-dot laser diodes," *IEEE Photonics Technology Letters* **11**, 1527-1529, 1999.
4. J. D. Thomson, H. D. Summers, P. J. Hulyer, P. M. Smowton, and P. Blood, "Determination of single-pass optical gain and internal loss using a multisection device," *Applied Physics Letters* **75**, 2527-2529, 1999.
5. P. Blood, G. M. Lewis, P. M. Smowton, H. Summers, J. Thomson, and J. Lutti, "Characterization of semiconductor laser gain media by the segmented contact method," *IEEE Journal of Selected Topics in Quantum Electronics* **9**, 1275-1282, 2003.
6. Joseph T.Verdeyen, *Laser Electronics*, 1995.
7. Oster, A; Erbert, G; Wenzel, H, "Gain spectra measurements by a variable stripe length method with current injection", *Electronics Letters* **33**, 864-866, 1997.
8. G. W. Wen, J. Y. Lin, H. X. Jiang, and Z. Zhen, "Quantum-confined Stark effects in semiconductor quantum dots" *Phys. Rev. B*, **52**, 5913ñ5922, 1995.
9. X. D. Huang, A. Stintz, H. Li, A. Rice, G. T. Liu, L. F. Lester, J. Cheng, and K. J. Malloy, "Bistable operation of a two-section 1.3-mu m InAs quantum dot laser - Absorption saturation and the quantum confined Stark effect," *IEEE Journal of Quantum Electronics* **37**, 414-417, 2001

10. P. W. Fry, I. E. Itskevich, D. J. Mowbray, M. S. Skolnick, J. J. Finley, J. A. Barker, E. P. O'Reilly, L. R. Wilson, I. A. Larkin, P. A. Maksym, M. Hopkinson, M. Al Khafaji, J. P. R. David, A. G. Cullis, G. Hill, and J. C. Clark, "Inverted electron-hole alignment in InAs-GaAs self-assembled quantum dots," *Physical Review Letters* **84**, 733-736, 2000
11. L. F. Lester, A. Stintz, H. Li, T. C. Newell, E. A. Pease, B. A. Fuchs, and K. J. Malloy, "Optical characteristics of 1.24-mu m InAs quantum-dot laser diodes," *IEEE Photonics Technology Letters* **11**, 931-933 1999.
12. G. T. Liu, A. Stintz, H. Li, T. C. Newell, A. L. Gray, P. M. Varangis, K. J. Malloy, and L. F. Lester, "The influence of quantum-well composition on the performance of quantum dot lasers using InAs/InGaAs dots-in-a-well (DWELL) structures," *IEEE J. Quantum Electron.* **36**, 1272-1279, 2000.
13. A. Stintz, G. T. Liu, A. L. Gray, R. Spillers, S. M. Delgado, and K. J. Malloy, ìCharacterization of InAs quantum dots in strained $In_xGa_{1-x}As$ quantum wells,î *J. Vac. Sci & Technol.* **B18**, 1496-1501, 2000.